# Efficient multiscale simulation of InGaN laser diodes

Michael Povolotskyi*, Benjamin Connors* and Benjamin Klein*
*Georgia Institute of Technology, 210 Technology Circle, Savannah GA 31407 USA Email: ben.klein@gtsav.gatech.edu

***Abstract*—We present an efficient 3D simulation method for a nitride-based visible light laser diode. The method involves the separation of the overall device simulation into coupled simplified models for the quantum wells, the $p-n$ junction, the bulk regions, and the thermal environment, each solved on a different mesh.**

## I. Simulation procedure

Drift-diffusion simulation of complex 3D laser structures is a time- and resource-intensive computational task. In order to accomplish a relatively fast 3D simulation of the laser diode, the laser simulation problem is separated into a set of sub-problems, each of which can be solved on a different spatial domain [1], [2]. The coupling between these sub-problems is generally weak and can be restricted to a subset of the points on the larger domain. The sub-problems are as follows, in order of increasing domain size:

- quantum well density of states, stimulated and spontaneous recombination in the $\mathbf{k} \cdot \mathbf{p}$ approximation [3];
- p-n junction recombination and optical gain in the quasi-equilibrium approximation;
- bulk region carrier transport in the unipolar drift current approximation;
- optical mode calculation and a photon rate equation;
- thermal transport simulation using the continuity equation for heat flux.

Each of these sub-problems is described in more detail below.

The quantum well density of states and recombination rates are calculated using a 6-band $\mathbf{k} \cdot \mathbf{p}$ solver including strain. The self-consistent electric potential (including the bending due to piezoelectric and spontaneous polarization fields) is passed to the $\mathbf{k} \cdot \mathbf{p}$ solver from the quasi-equilibrium $p$-$n$ junction solver described in the next paragraph. The Hamiltonian is discretized using the real-space finite difference procedure, and solved to obtain the eigenstates in the well. The bound state energies and wavefunctions are used in conjunction with the electron and hole quasi-Fermi levels passed from the $p$-$n$ junction solver to calculate the dark recombination, spontaneous recombination, and optical gain of the quantum well.

The $p$-$n$ junction is simulated using a set of parallel 1D models in the quasi-equilibrium approximation. Each 1D model represents a patch of the $p$-$n$ junction, as shown in Fig. 1. The recombination and gain of a $p$-$n$ junction patch are calculated as follows. Starting from equilibrium, the strain and polarization of the $p$-$n$ junction region are calculated, and the nonlinear 1D Poisson equation with self-consistent electron and hole concentrations is solved in the growth direction using the finite-element discretization procedure [4]. Although the $p$-$n$ junction requires fine spatial meshing, the use of 1D models greatly reduces the problem size, while neglecting current spreading in the active layer. The bias applied to the patch is increased in steps, and the electron and hole quasi-Fermi levels are assumed to be spatially invariant and equal to the $n$-side and $p$-side Fermi levels, respectively. The nonlinear Poisson equation is solved again for each bias step. The dark recombination, spontaneous recombination, and optical gain of the active layer patch are calculated and stored in a look-up table for a range of applied bias conditions and temperatures. This data is later used as described in the next paragraph.

The carrier transport in the bulk regions of the device bounding the active region are modeled in 3D, in order to obtain current spreading and series resistance in complex laser diode structures. The drift continuity equation is solved for the majority carrier population using the finite element discretization procedure. At the boundaries of the $p$-$n$ junction region, the current through each $p$-$n$ junction patch is obtained from the recombination rates and optical gain from the look-up table described above, along with the photon number from the photon rate equation:

$$j = e(R^{\mathrm{dark}} + R^{\mathrm{rad}} + \gamma N G), \tag{1}$$

where $R^{\mathrm{dark/rad}}$ are the dark/radiative spontaneous recombination rates, $N$ is the number of photons in the resonator, $G$ and $\gamma$ are the modal gain and the overlap factor, respectively. The optical mode calculation, necessary to calculate modal overlap factors and the photon lifetime of the lasing mode, can be carried out using a variety of approaches, e.g. [5]. The photon rate equation is given by many authors, e.g. [6].

The thermal transport simulation is modeled using a thermal continuity equation [7]. Heat generation due to Joule heating is calculated in the bulk regions, while the heat generation in the $p$-$n$ junction region is calculated from energy balance considerations: the total power dissipated in the $p$-$n$ junction region minus the power loss due to optical recombination. The thermal continuity equation is discretized using finite elements, and the mesh is a superset of the mesh used for bulk carrier transport.

Self-consistency between all the layers of models is achieved by iteration. The active layer and bulk transport are solved simultaneously using the Newton method [8], while the

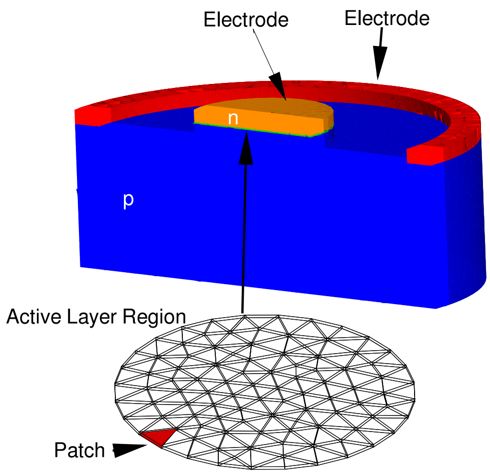


Fig. 1. Schematic plot of the simulated VCSEL structure. The mesh in active layer region region is shown.

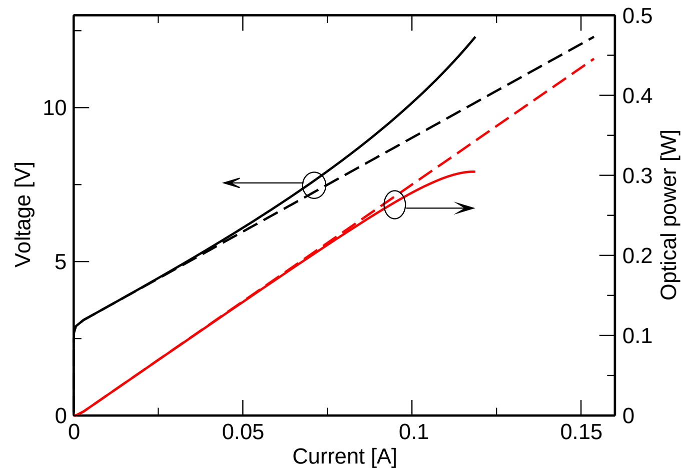


Fig. 2. Voltage vs. current and output power vs. current dependencies calculated with (solid lines) and without (dashed lines) thermal modelling.

photon rate equation and the thermal transport are solved in outer Gummel iterations.

## II. Simulation Example

As the application example we consider an InGaN/GaN VCSEL structure (see Fig. 1). The active layers of the laser consists of a $In_{0.19}Ga_{0.81}N$ quantum well of 3nm thickness surrounded by two $In_{0.02}Ga_{0.98}N$ barriers of 5nm thickness. The active layer is located between $n$ and $p$ doped GaN bulk regions. The device is surrounded by an insulating GaN layer. A voltage is applied through the contacts, located at the top of the $n$ and $p$ layers.

The IV characteristic of the device is shown in Fig. 2. As the applied voltage goes above 2.5V, the current increases exponentially, due to the diode action of the active layer. As the applied voltage goes above 3V, the current increases linearly. This linear trend in the IV is due to the clamping of the voltage drop across the active layer above laser threshold; additional applied voltage is dropped across the bulk layers, which act as series resistors. A similar linear trend is found in the output optical power dependence on current because above threshold, the current that passes through the active layer is mostly due to the stimulated emission process.

As the current reaches the 0.05A value, the thermal effects become important. As one sees from Fig. 3, the active layer is heated up to 380K, when the current reaches a value of 0.1A at 10V bias. As a consequence, at such high biases the gain peak of the active layer shifts away from the cavity resonance, and current and output power go to saturation. For comparison we plot the simulation results obtained neglecting the device heating (Fig. 2, dashed lines) that show a constant linear growth of the output power with the applied voltage.

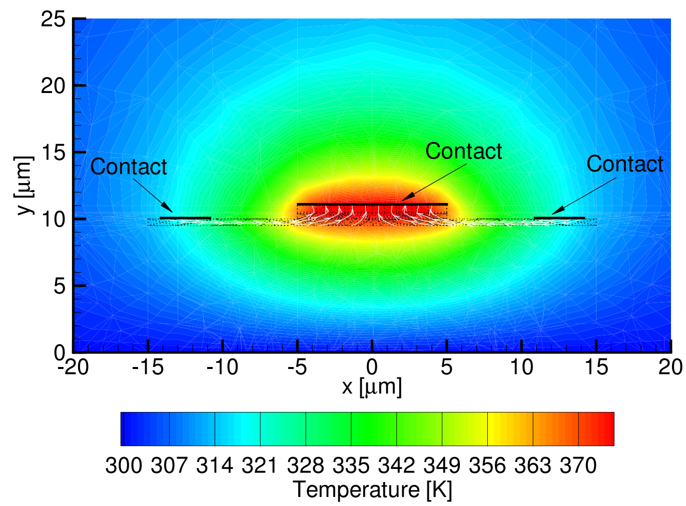


Fig. 3. Temperature distribution over the $xz$ plane and electric current lines at 10V bias. The mesh in the current conducting device region (black lines) is shown.

## References

[1] I. Y. Evstratov, V. Mymrin, S. Y. Karpov, and Y. N. Makarov, "Current crowding effects on blue LED operation," *Phys. Stat. Sol*, no. 6, p. 1645, 2006.

[2] M. Osiński, V. A. Smagley, M. Lu, G. A. Smolyakov, P. G. Eliseev, B. P. Riely, P. H. Shen, and G. J. Simonis, "Self-consistent calculation of current self-distribution effect in GaAs-AlGaAs oxide-confined VCSELs," *IEEE J. Sel. Topics Quantum Electron.*, vol. 9, p. 1422, 2003.

[3] S. L. Chuang and C. S. Chang, "k · p method for strained wurtzite semiconductors," *Phys. Rev. B*, vol. 54, no. 4, p. 2491.

[4] "libMesh, a framework for the numerical simulation of partial differential equations using arbitrary unstructured discretizations on serial and parallel platforms," on-line, http://libmesh.sourceforge.net/.

[5] B. Klein, L. F. Register, and H. K., "Self-consistent green's function approach to the analysis of dielectrically apertured vertical-cavity surface-emitting lasers," *Appl. Phys. Letters*, vol. 73, p. 3324, 1998.

[6] M. A. Alam, M. S. Hybertsen, R. K. Smith, and G. A. Baraff, "Simulation of semiconductor quantum well lasers," *IEEE Trans. Electron Devices*, vol. 47, p. 1917, 2000.

[7] G. K. Wachutka, "Rigorous thermodynamic treatment of heat generation and conduction in semiconductor device modeling," *IEEE Trans. on Computer Aided Design*, vol. 9, p. 1141, 1990.

[8] "Portable, Extensible Toolkit for Scientific Computation (PETSc) ," on-line, http://www-unix.mcs.anl.gov/petsc/petsc-2/.